



# Pathways of N<sub>2</sub>O production by marine ammonia-oxidizing archaea determined from dual-isotope labeling

Xianhui S. Wan<sup>a,1</sup>, Lei Hou<sup>b,c</sup>, Shuh-Ji Kao<sup>b</sup>, Yao Zhang<sup>b</sup> , Hua-Xia Sheng<sup>b</sup>, Hui Shen<sup>b</sup>, Senwei Tong<sup>b</sup> , Wei Qin<sup>c</sup> , and Bess B. Ward<sup>a,1</sup>

Edited by Donald Canfield, Syddansk Universitet, Odense M, Denmark; received December 13, 2022; accepted February 7, 2023

The ocean is a net source of the greenhouse gas and ozone-depleting substance, nitrous oxide (N<sub>2</sub>O), to the atmosphere. Most of that N<sub>2</sub>O is produced as a trace side product during ammonia oxidation, primarily by ammonia-oxidizing archaea (AOA), which numerically dominate the ammonia-oxidizing community in most marine environments. The pathways to N<sub>2</sub>O production and their kinetics, however, are not completely understood. Here, we use <sup>15</sup>N and <sup>18</sup>O isotopes to determine the kinetics of N<sub>2</sub>O production and trace the source of nitrogen (N) and oxygen (O) atoms in N<sub>2</sub>O produced by a model marine AOA species, *Nitrosopumilus maritimus*. We find that during ammonia oxidation, the apparent half saturation constants of nitrite and N<sub>2</sub>O production are comparable, suggesting that both processes are enzymatically controlled and tightly coupled at low ammonia concentrations. The constituent atoms in N<sub>2</sub>O are derived from ammonia, nitrite, O<sub>2</sub>, and H<sub>2</sub>O via multiple pathways. Ammonia is the primary source of N atoms in N<sub>2</sub>O, but its contribution varies with ammonia to nitrite ratio. The ratio of <sup>45</sup>N<sub>2</sub>O to <sup>46</sup>N<sub>2</sub>O (i.e., single or double labeled N) varies with substrate ratio, leading to widely varying isotopic signatures in the N<sub>2</sub>O pool. O<sub>2</sub> is the primary source for O atoms. In addition to the previously demonstrated hybrid formation pathway, we found a substantial contribution by hydroxylamine oxidation, while nitrite reduction is an insignificant source of N<sub>2</sub>O. Our study highlights the power of dual <sup>15</sup>N-<sup>18</sup>O isotope labeling to disentangle N<sub>2</sub>O production pathways in microbes, with implications for interpretation of pathways and regulation of marine N<sub>2</sub>O sources.

nitrous oxide | ammonia-oxidizing archaea | dual isotope | marine N<sub>2</sub>O production pathways | kinetics

Ammonia-oxidizing archaea (AOA) are ubiquitous and abundant members of the marine plankton; they are almost exclusively responsible for ammonia oxidation in the world ocean (1, 2). Globally, over 80% of marine nitrous oxide (N<sub>2</sub>O) is estimated to be produced as a side product of ammonia oxidation (3–5), indicating a dominant role of marine AOA in determining N<sub>2</sub>O distribution and its flux from ocean to atmosphere. Compared to their bacterial counterparts, ammonia-oxidizing bacteria (AOB), marine AOA lack the genes encoding the known bacterial machineries for N<sub>2</sub>O production (6) and exhibit lower N<sub>2</sub>O yield (7–9), implying distinct mechanisms of N<sub>2</sub>O production between AOA and AOB (10–12). The marine AOA demonstrate significantly higher affinity toward total ammonia (NH<sub>3</sub> plus NH<sub>4</sub><sup>+</sup>, hereafter referred to as NH<sub>4</sub><sup>+</sup>) for ammonia oxidation during nitrite (NO<sub>2</sub><sup>-</sup>) production than AOB (2), but the cellular kinetics of N<sub>2</sub>O production have not been explored. Hydroxylamine (NH<sub>2</sub>OH) and nitric oxide (NO) have been identified as key intermediates in AOA metabolism (13–15), implying multiple potential pathways for N<sub>2</sub>O production as both NH<sub>2</sub>OH and NO are likely precursors of N<sub>2</sub>O. However, the explicit pathways of archaeal N<sub>2</sub>O production are still incompletely known and remain controversial (10–12). The hybrid N<sub>2</sub>O formation pathway (in which the two N atoms in N<sub>2</sub>O are derived from different sources via the abiotic reaction between NH<sub>2</sub>OH and NO) has been experimentally demonstrated and is considered the dominant pathway for N<sub>2</sub>O production in AOA cultures and natural environments (Fig. 1A) (10–12). Other AOA pathways may include N<sub>2</sub>O production via NO<sub>2</sub><sup>-</sup> reduction at low pH (16) and a novel NO dismutation pathway in marine AOA under anaerobic conditions (17). In contrast, no experimental evidence that AOA can directly convert NH<sub>2</sub>OH to N<sub>2</sub>O via NH<sub>2</sub>OH oxidation, either enzymatically or abiotically, has been reported. It is important to determine which pathways occur during archaeal ammonia oxidation and which are relevant in various environmental conditions because 1) the pathway and rate of N<sub>2</sub>O production might vary with NH<sub>4</sub><sup>+</sup> and NO<sub>2</sub><sup>-</sup> availability, as both are involved in N<sub>2</sub>O formation; and 2) different sources of N and O used by AOA to produce N<sub>2</sub>O may impart distinct isotope signatures, which are used to deduce the sources of N<sub>2</sub>O in natural and man-made systems.

Elucidation of all potential sources of N<sub>2</sub>O, however, remains a challenging task. To date, most investigations on AOA N<sub>2</sub>O production pathways have focused on the source

## Significance

Ammonia-oxidizing archaea (AOA) are the major source of marine nitrous oxide (N<sub>2</sub>O); however, the cellular kinetics and pathways of archaeal N<sub>2</sub>O production remain unclear. We characterize N<sub>2</sub>O production kinetics of a model marine AOA species *Nitrosopumilus maritimus* at low ammonia concentrations and quantify the relative contributions of multiple N<sub>2</sub>O production pathways using dual <sup>15</sup>N-<sup>18</sup>O isotope labeling. We provide direct evidence for the enzymatic regulation of N<sub>2</sub>O production by AOA. We found hydroxylamine oxidation contributes substantially to N<sub>2</sub>O production, which had not been previously recognized, and that nitrite reduction is not a significant source of N<sub>2</sub>O. These findings are important for the interpretation of pathways and regulation of N<sub>2</sub>O production in the ocean.

Author contributions: X.S.W., W.Q., and B.B.W. designed research; X.S.W., L.H., H.-X.S., H.S., and S.T. performed research; S.-J.K., and Y.Z. contributed new reagents/analytic tools; X.S.W., L.H., W.Q., and B.B.W. analyzed data; and X.S.W. and B.B.W. wrote the paper with input from all authors.

The authors declare no competing interest.

This article is a PNAS Direct Submission.

Copyright © 2023 the Author(s). Published by PNAS. This article is distributed under [Creative Commons Attribution-NonCommercial-NoDerivatives License 4.0 \(CC BY-NC-ND\)](https://creativecommons.org/licenses/by-nc-nd/4.0/).

<sup>1</sup>To whom correspondence may be addressed. Email: xianhuiw@princeton.edu or bbw@princeton.edu.

This article contains supporting information online at <https://www.pnas.org/lookup/suppl/doi:10.1073/pnas.2220697120/-/DCSupplemental>.

Published March 8, 2023.

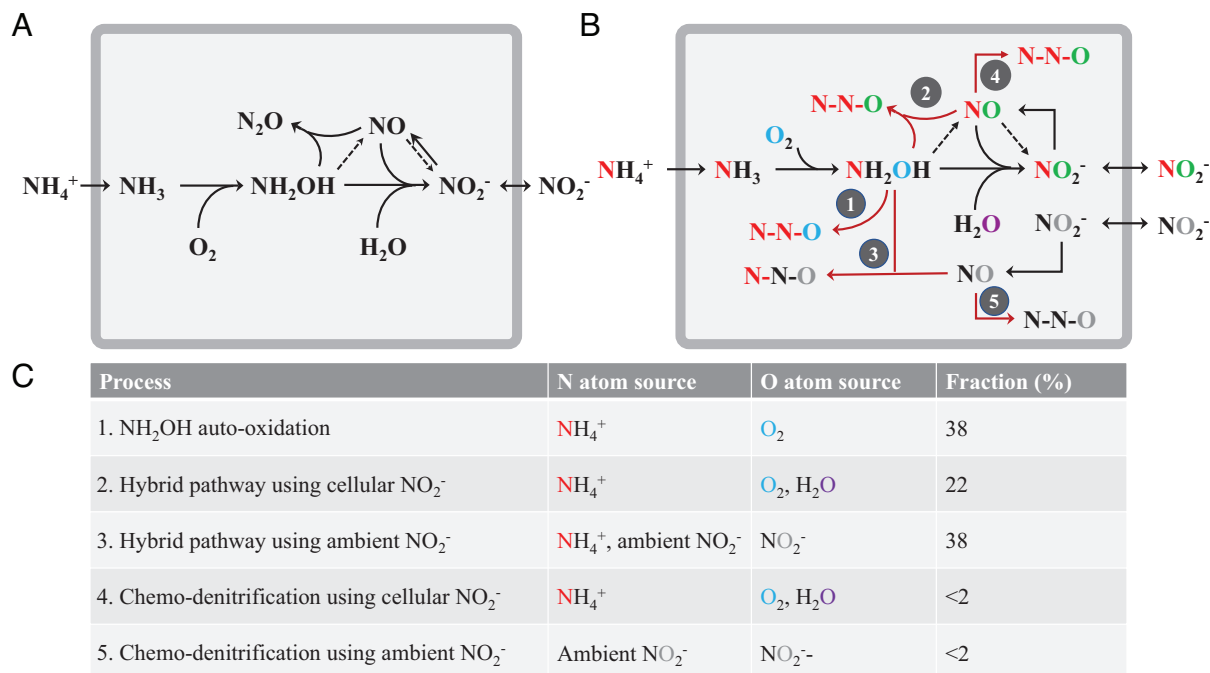


**Fig. 1.** Summary of N<sub>2</sub>O production pathways during marine archaeal ammonia oxidation. (A) The hybrid pathway, which combines one N atom from NH<sub>2</sub>OH and one from nitrite (either ambient or newly produced inside the cell), has been observed previously (10–12). Black arrows represent known pathways for N atoms; dashed pathways represent hypothesized pathways involving NO. (B) Potential N<sub>2</sub>O pathways and the N and O atom sources identified in the current study. Five N<sub>2</sub>O pathways are identified: 1) NH<sub>2</sub>OH oxidation; 2) hybrid pathway a: NH<sub>2</sub>OH reaction with NO that was sourced from the reduction of newly produced NO<sub>2</sub><sup>-</sup>; 3) hybrid pathway b: NH<sub>2</sub>OH reaction with NO that was sourced from ambient NO<sub>2</sub><sup>-</sup>; 4) reduction of newly produced NO<sub>2</sub><sup>-</sup>; and 5) reduction of ambient NO<sub>2</sub><sup>-</sup>. Color of the N and O atoms depicts the sources: red and black denote N atoms from NH<sub>4</sub><sup>+</sup> and ambient NO<sub>2</sub><sup>-</sup>, respectively; blue, purple, and gray denote O atoms from O<sub>2</sub>, H<sub>2</sub>O, and ambient NO<sub>2</sub><sup>-</sup>, respectively; green represents O atoms of newly produced NO<sub>2</sub><sup>-</sup>, which is a mixture of H<sub>2</sub>O and O<sub>2</sub>. The gray square denotes the membrane and periplasmic space of the AOA cell. The black arrows represent the ammonia oxidation pathway, the red arrows show the potential N<sub>2</sub>O production processes, and the dashed arrows indicate potential pathways that are unresolved in our study. (C) Summary of the N, O atom sources of N<sub>2</sub>O and the fractional contribution of each pathway during marine archaeal ammonia oxidation with initial NH<sub>4</sub><sup>+</sup>: NO<sub>2</sub><sup>-</sup> ratio of 1:1.

of the nitrogen (N) atoms (13, 16–18). However, using N isotopes alone is insufficient to distinguish multiple N<sub>2</sub>O production pathways that occur simultaneously and to quantitatively estimate the relative contribution of each pathway. For instance, the <sup>15</sup>N-NH<sub>4</sub><sup>+</sup> isotope labeling approach cannot completely distinguish N<sub>2</sub>O production through NH<sub>2</sub>OH oxidation, hybrid formation, or NO<sub>2</sub><sup>-</sup> reduction, because all these precursors of N<sub>2</sub>O could ultimately be sourced from NH<sub>4</sub><sup>+</sup> during ammonia oxidation. The <sup>18</sup>O-labeling approach provides an independent avenue to identify the source of N<sub>2</sub>O by tracking the oxygen (O) atom in N<sub>2</sub>O. A few studies have used <sup>18</sup>O-H<sub>2</sub>O to show that the O atom in N<sub>2</sub>O can be partly derived from H<sub>2</sub>O in lab culture and field studies (9, 19, 20). However, the alternative sources of the O atom in N<sub>2</sub>O are still unknown. Importantly, because the O atom source differs among the various N-containing precursors, i.e., NH<sub>2</sub>OH, NO<sub>2</sub><sup>-</sup>, and NO, dual <sup>15</sup>N and <sup>18</sup>O isotope labeling is a powerful method to disentangle the complex and interconnected N<sub>2</sub>O production pathways in AOA. In this study, using a model marine AOA species *Nitrosopumilus maritimus* strain SCM1 (hereafter refer to as SCM1), we conducted a comprehensive set of dual-isotope labeling incubation experiments to systematically investigate N<sub>2</sub>O production kinetics and the associated pathways during archaeal ammonia oxidation under various substrate conditions (SI Appendix, Table S1).

## Results and Discussion

**Kinetics of N<sub>2</sub>O Production during Archaeal Ammonia Oxidation.** Marine AOA have a remarkably high affinity for NH<sub>4</sub><sup>+</sup>, which is consistent with their dominant role in ammonia oxidation to NO<sub>2</sub><sup>-</sup> in oligotrophic marine environments (2). However, the

effect of NH<sub>4</sub><sup>+</sup> concentrations on N<sub>2</sub>O production by AOA remains unknown. If N<sub>2</sub>O is primarily generated via abiotic hybrid reactions between intermediates of archaeal ammonia oxidation, N<sub>2</sub>O production by AOA may not follow normal enzyme kinetics. We found that both NO<sub>2</sub><sup>-</sup> and N<sub>2</sub>O production rates varied with NH<sub>4</sub><sup>+</sup> concentration (Experiment 1) and both followed Michaelis-Menten-type kinetics (Fig. 2 A and B). The apparent half saturation constants ( $K_{m(\text{app})}$ ) for NO<sub>2</sub><sup>-</sup> production (220 ± 50 nmol L<sup>-1</sup> NH<sub>4</sub><sup>+</sup>) were comparable to those that were previously determined for ammonia (132 nmol L<sup>-1</sup> NH<sub>4</sub><sup>+</sup>) and oxygen uptake (133 nmol L<sup>-1</sup> NH<sub>4</sub><sup>+</sup>), suggesting all essential enzymatic steps for ammonia oxidation and respiration are highly efficient and tightly coupled at low ammonia concentrations in marine AOA. Likewise, although the maximum rate ( $V_{\text{max}}$ ) for N<sub>2</sub>O production (0.97 ± 0.02 amol N cell<sup>-1</sup> d<sup>-1</sup>) was more than three orders of magnitude lower than that for NO<sub>2</sub><sup>-</sup> production (7.14 ± 0.25 fmol N cell<sup>-1</sup> d<sup>-1</sup>),  $K_{m(\text{app})}$  values for the two rates were comparably low. The comparable  $K_{m(\text{app})}$  values for ammonia during NO<sub>2</sub><sup>-</sup> and N<sub>2</sub>O production imply that both are controlled by enzyme activity in SCM1 at low NH<sub>4</sub><sup>+</sup> concentrations. This implies that enzyme activity provides the key intermediates NH<sub>2</sub>OH and NO for both NO<sub>2</sub><sup>-</sup> and N<sub>2</sub>O production, i.e., there is no separate completely abiotic reaction that is responsible for N<sub>2</sub>O production. The  $K_{m(\text{app})}$  for N<sub>2</sub>O production is four orders of magnitude lower than the  $K_m$  reported for NO production by SCM1 measured during ammonia oxidation (measured at >2 mol L<sup>-1</sup> NH<sub>4</sub><sup>+</sup>) (14). Therefore, the supply of NO is unlikely to be a limiting factor in determining the kinetics of N<sub>2</sub>O production, implying a critical role for NH<sub>2</sub>OH in determining the observed kinetics.

NH<sub>2</sub>OH is enzymatically produced by ammonia monooxygenase and rapidly converted to NO<sub>2</sub><sup>-</sup> (15). The tight coupling of its

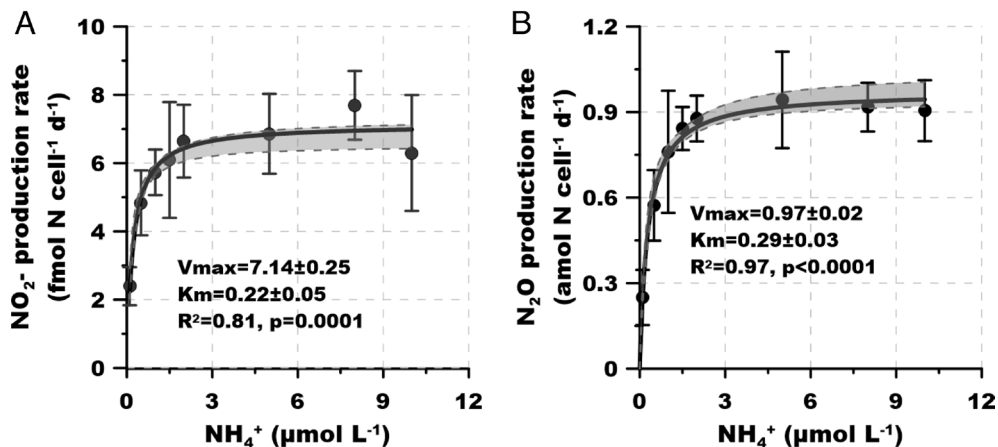


**Fig. 2.** Experiment 1. Kinetics of ammonia oxidation and  $\text{N}_2\text{O}$  production by SCM1. (A) Michaelis-Menten-type plot of substrate-dependent rate of ammonia oxidation to  $\text{NO}_2^-$  (normalized to per cell per day). (B) Michaelis-Menten plot of substrate-dependent rate of  $\text{N}_2\text{O}$  production. Error bars represent SD from triplicate samples. The black lines and gray shadows show the Michaelis-Menten type regressions and the 95% CIs, respectively.

production and consumption in AOA species at low  $\text{NH}_4^+$  concentrations results in its limiting conversion to  $\text{N}_2\text{O}$  as a side product. However, a small fraction of  $\text{NH}_2\text{OH}$  can escape from being oxidized by the enzymatic reaction, providing the key precursor for  $\text{N}_2\text{O}$  production. For example, only 0.46% of  $\text{NH}_2\text{OH}$  was released during ammonia oxidation by the AOA *Nitrososphaera gargensis* even at very high  $\text{NH}_4^+$  concentrations [2 mmol  $\text{L}^{-1}$  (21)], which is one to two orders of magnitude lower than the reported  $\text{NO}$  accumulation ratio during ammonia oxidation by SCM1 (14). The similarly high affinities (low  $K_m$ ) for  $\text{NO}_2^-$  and  $\text{N}_2\text{O}$  production further suggest that both kinetics were determined by the  $\text{NH}_2\text{OH}$  supply; if the conversion of  $\text{NH}_2\text{OH}$  to  $\text{NO}_2^-$  was the rate-limiting step, the production of  $\text{N}_2\text{O}$  should increase continuously with the accumulation of  $\text{NH}_2\text{OH}$ . These results suggest that the SCM1-like marine AOA effectively use the trace level  $\text{NH}_4^+$  in the vast N-depleted ocean for both  $\text{NO}_2^-$  and  $\text{N}_2\text{O}$  generation, providing direct evidence for the capability of marine AOA to dominate  $\text{N}_2\text{O}$  production in the ocean and its subsequent release to the atmosphere.

**Impact of  $\text{NH}_4^+ : \text{NO}_2^-$  Ratio on Pathways of  $\text{N}_2\text{O}$  Production.** Both  $\text{NH}_4^+$  and  $\text{NO}_2^-$  are involved in  $\text{N}_2\text{O}$  production by AOA (9, 18), but the rates and pathways might vary depending on relative substrate availability. Therefore, we investigated  $\text{N}_2\text{O}$  production under a wide range of  $^{15}\text{NH}_4^+ : ^{14}\text{NO}_2^-$  ratios (from

0.05 to 10) (Experiments 1 and 2). The ratio of single labeled  $\text{N}_2\text{O}$  to double labeled  $\text{N}_2\text{O}$  ( $^{45}\text{N}_2\text{O} : ^{46}\text{N}_2\text{O}$ ) decreased from  $5.82 \pm 2.58$  to  $0.37 \pm 0.05$  as the  $^{15}\text{NH}_4^+ : ^{14}\text{NO}_2^-$  ratio increased from 0.05 to 10 (Fig. 3A and *SI Appendix, Fig. S1*). This dependence on substrate ratio indicates that  $^{45}\text{N}_2\text{O} : ^{46}\text{N}_2\text{O}$  ratio is not a constant but is highly variable and implies that more than one pathway contributes to  $\text{N}_2\text{O}$  production in AOA. The strong and significant correlation ( $R^2 = 0.97$ ,  $P < 0.0001$ ) between the  $^{45}\text{N}_2\text{O} : ^{46}\text{N}_2\text{O}$  ratio and substrate  $^{15}\text{NH}_4^+ : ^{14}\text{NO}_2^-$  ratio implies that the relative contributions of different pathways to  $\text{N}_2\text{O}$  production and the source of the N atoms in  $\text{N}_2\text{O}$  should vary with  $\text{NH}_4^+ : \text{NO}_2^-$  ratio in the environment (Fig. 3B).

$\text{NH}_4^+$  and  $\text{NO}_2^-$  are highly dynamic nitrogen cycle components that rarely accumulate in the global ocean. However,  $\text{NH}_4^+$  and  $\text{NO}_2^-$  can accumulate in specific regions (e.g., oxygen minimum zones and eutrophic waters) and depths (e.g.,  $\text{NH}_4^+$  maximum, primary  $\text{NO}_2^-$  maximum), leading to substantial variation of  $\text{NH}_4^+ : \text{NO}_2^-$  ratio in these biogeochemically active marine environments (22). Our data indicate that  $\text{N}_2\text{O}$  can be produced via distinct pathways by marine AOA and sourced from different N atoms in waters with different ratios of  $\text{NH}_4^+ : \text{NO}_2^-$ , even though the main source process is always archaeal ammonia oxidation. For example, at the primary  $\text{NO}_2^-$  maximum where  $\text{NO}_2^-$  accumulates, the low  $\text{NH}_4^+ : \text{NO}_2^-$  ratio might lead to the higher contribution of  $\text{NO}_2^-$  to  $\text{N}_2\text{O}$  production via the hybrid pathway. In

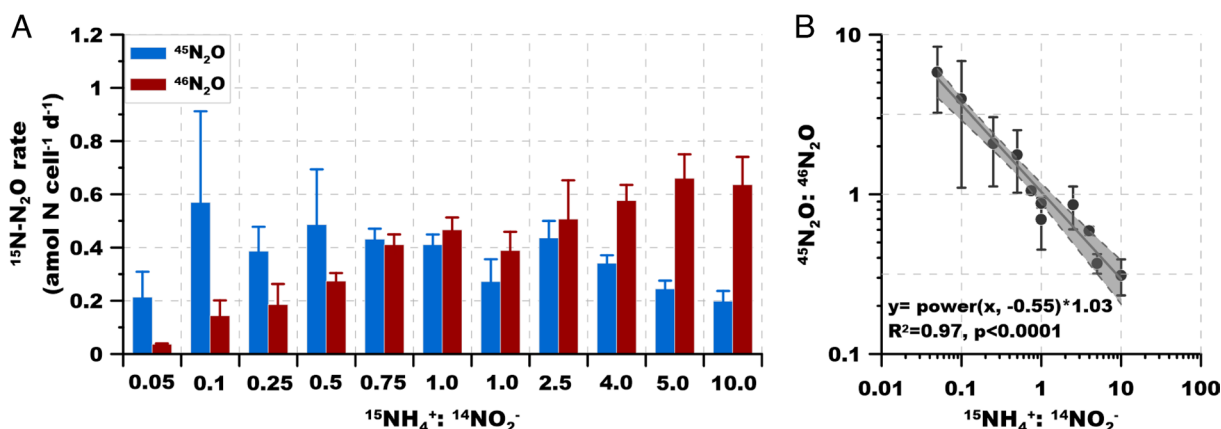


**Fig. 3.** Experiment 2.  $^{15}\text{N}$ - $\text{N}_2\text{O}$  production and isotope composition under different  $^{15}\text{NH}_4^+ : ^{14}\text{NO}_2^-$  ratios. (A)  $^{45}\text{N}_2\text{O}$  (single labeled) and  $^{46}\text{N}_2\text{O}$  (double labeled) production rate under different  $^{15}\text{NH}_4^+$  and  $^{14}\text{NO}_2^-$  concentrations (normalized to per cell per day). All of the  $^{45}\text{N}_2\text{O}$  represents hybrid formation. (B) Regression between  $^{45}\text{N}_2\text{O} : ^{46}\text{N}_2\text{O}$  production rate against  $^{15}\text{NH}_4^+ : ^{14}\text{NO}_2^-$  concentration ratio. Error bars represent SD from triplicate samples.

contrast, at the  $\text{NH}_4^+$  maximum and certain hotspots of  $\text{NH}_4^+$  supply such as zooplankton excretion or decay of phytoplankton blooms (23),  $\text{NH}_4^+$  would dominate  $\text{N}_2\text{O}$  formation under the elevated  $\text{NH}_4^+:\text{NO}_2^-$  ratio. These findings provide new insights in interpreting the natural abundance isotope signature of  $\text{N}_2\text{O}$  in the water column of the global oligotrophic oceans, where a subsurface dual-isotope minimum is consistently observed and has been widely interpreted as resulting from  $\text{N}_2\text{O}$  production via nitrifier-denitrification (24–27). These new data would suggest, however, that low  $\text{NH}_4^+:\text{NO}_2^-$  ratio (i.e., relatively higher  $\text{NO}_2^-$  concentration) would also lead to the observed dual-isotope minimum by the incorporation of more isotopically depleted  $\text{NO}_2^-$  by the hybrid pathway during the ammonia oxidation process.

Our results are also important for the interpretation of isotope labeling patterns observed in isotope tracer experiments in the ocean, where production of  $^{45}\text{N}_2\text{O}$  has been generally attributed to the hybrid  $\text{N}_2\text{O}$  formation pathway (one N from  $\text{NH}_4^+$ , one N from  $\text{NO}_2^-$ ). We suggest that  $^{46}\text{N}_2\text{O}$  could also be partially hybrid, from the combination of  $^{15}\text{NH}_4^+$  and newly produced  $^{15}\text{NO}_2^-$ . The contribution of the hybrid pathway would be underestimated by ignoring  $^{46}\text{N}_2\text{O}$  production. However, our results cannot fully explain the high fraction of  $^{45}\text{N}_2\text{O}$  production (i.e., >70%) in the ocean (24, 28–30), nor the finding that the % $^{46}\text{N}_2\text{O}$  is insensitive to short-term experimental  $\text{NO}_2^-$  enrichment (31) (comparison to field observations; *SI Appendix, Text 1*). Nevertheless, the variable  $\text{N}_2\text{O}$  atom composition by SCM1 under different  $\text{NH}_4^+:\text{NO}_2^-$  ratio provides new insights into marine  $\text{N}_2\text{O}$  pathways and interpretation of its isotope composition. These pathways and the relative contributions of N and O from multiple sources are explored in experiments described below.

**Contributions of  $\text{NH}_4^+$  and  $\text{NO}_2^-$  to  $\text{N}_2\text{O}$  Production.** The potential pathways and relative contributions of the two substrates,  $\text{NH}_4^+$  and  $\text{NO}_2^-$ , via various pathways of  $\text{N}_2\text{O}$  formation in AOA were explored using multiple tracer combinations (Experiment 3).  $\text{NH}_4^+$  and  $\text{NO}_2^-$  concentrations were controlled by adding the substrates to cells that had first been washed and resuspended in substrate-free fresh medium. When  $^{15}\text{NH}_4^+$  was added without  $^{14}\text{NO}_2^-$ , double labeled  $^{46}\text{N}_2\text{O}$  was the main product ( $93.4 \pm 10.1\%$  of the total labeled  $\text{N}_2\text{O}$  production rate) (Fig. 4A).  $^{15}\text{NH}_4^+$  was the only N source in the experiment, so the small production of  $^{45}\text{N}_2\text{O}$  (6.6% of the total labeled  $\text{N}_2\text{O}$  production) can be attributed to trace amounts of intracellular  $^{14}\text{NH}_4^+$  and/or  $^{14}\text{NO}_2^-$ , or to carry over from the inoculum. When equimolar amounts of

$^{15}\text{NH}_4^+$  and  $^{14}\text{NO}_2^-$  were provided, the fractional contribution of  $^{45}\text{N}_2\text{O}$  increased to 28.9%, indicating that ambient  $\text{NO}_2^-$  is involved in  $^{45}\text{N}_2\text{O}$  production, although the labeled  $\text{N}_2\text{O}$  pool was still primarily  $^{46}\text{N}_2\text{O}$ . This hybrid  $\text{N}_2\text{O}$  formation indicates involvement of ambient  $\text{NO}_2^-$  in  $\text{N}_2\text{O}$  production, but the process varies among AOA strains (18) and with substrate ratio (Fig. 3B). Newly produced (presumably intracellular, or at least in the pseudo-periplasmic space) and ambient  $\text{NO}_2^-$  might both be involved in  $\text{N}_2\text{O}$  hybrid formation (pathways 2, 3 in Fig. 1B). Total labeled  $\text{N}_2\text{O}$  (combined  $^{45}\text{N}_2\text{O}$  and  $^{46}\text{N}_2\text{O}$ ) production rate in the  $^{15}\text{NH}_4^+$  tracer incubation ( $8.7 \pm 0.7 \text{ nmol N L}^{-1} \text{ d}^{-1}$ , Fig. 4A) was comparable to the rate in the  $^{15}\text{NH}_4^+ + ^{14}\text{NO}_2^-$  incubation ( $9.6 \pm 1.5 \text{ nmol N L}^{-1} \text{ d}^{-1}$ , Fig. 4B), indicating no discernible difference between the effects of ambient and newly produced  $\text{NO}_2^-$  on  $\text{N}_2\text{O}$  production rate by SCM1.

$^{15}\text{N}$ -labeled  $\text{N}_2\text{O}$  production from  $^{15}\text{NO}_2^-$  tracer was negligible ( $0.3 \pm 0.2 \text{ nmol N L}^{-1} \text{ d}^{-1}$ ) in the absence of  $\text{NH}_4^+$  (Fig. 4C). By comparison, when  $^{14}\text{NH}_4^+$  was added with  $^{15}\text{NO}_2^-$ , the  $^{15}\text{N}$ -labeled  $\text{N}_2\text{O}$  production rate increased significantly to  $2.6 \pm 0.3 \text{ nmol N L}^{-1} \text{ d}^{-1}$  ( $P < 0.001$ ), which is strong evidence for a hybrid  $\text{N}_2\text{O}$  formation mechanism that involves both intermediates from ammonia oxidation and  $\text{NO}_2^-$  reduction (Fig. 4D). It is not surprising that  $\text{N}_2\text{O}$  production rate decreased greatly in the absence of  $\text{NH}_4^+$ , as  $\text{NH}_4^+$  is the substrate for energy generation and the source of the key  $\text{N}_2\text{O}$  precursor  $\text{NH}_2\text{OH}$ . Thus,  $\text{N}_2\text{O}$  can be produced from  $\text{NH}_4^+$  alone in the absence of  $\text{NO}_2^-$ , but  $\text{N}_2\text{O}$  cannot be produced from  $\text{NO}_2^-$  alone. When  $\text{NH}_4^+$  is present, however,  $\text{NO}_2^-$  contributes to  $\text{N}_2\text{O}$  formation via a hybrid pathway. In contrast to the  $^{15}\text{NH}_4^+$  tracer experiment,  $^{45}\text{N}_2\text{O}$  dominated the  $^{15}\text{N}$ - $\text{N}_2\text{O}$  pool in the  $^{15}\text{NO}_2^- + ^{14}\text{NH}_4^+$  incubation ( $92.1 \pm 16.8\%$ ). The small fraction ( $7.9 \pm 3.4\%$ ) of  $^{46}\text{N}_2\text{O}$  detected in this treatment indicated a minor contribution of the chemo-denitrification-like pathway (i.e., both N atoms from  $\text{NO}_2^-$ , pathways 4, 5 in Fig. 1B) to  $\text{N}_2\text{O}$  production (Fig. 4D) (13). However, the  $^{46}\text{N}_2\text{O}$  production rate from  $^{15}\text{NO}_2^-$  measured here was two orders of magnitude lower than rates measured when external oxygen was exhausted ( $5$  to  $22 \text{ nmol L}^{-1} \text{ h}^{-1}$ ) (17), indicating production of  $\text{N}_2\text{O}$  in AOA by the proposed  $\text{NO}_2^-$  reduction- $\text{NO}$  dismutation pathway is restricted to anoxic conditions.

**The Role of  $\text{NH}_2\text{OH}$  as Key Precursor for  $\text{N}_2\text{O}$  Production.** Although  $\text{NH}_2\text{OH}$  is not an important N source in the marine environment (its reactivity guarantees a very low ambient concentration) (32), it is a critical intracellular intermediate in archaeal ammonia oxidation and  $\text{N}_2\text{O}$  production. Experiments using  $^{15}\text{NH}_2\text{OH}$  and  $^{15}\text{NO}_2^- + ^{14}\text{NH}_2\text{OH}$  were used to explore the pathways by

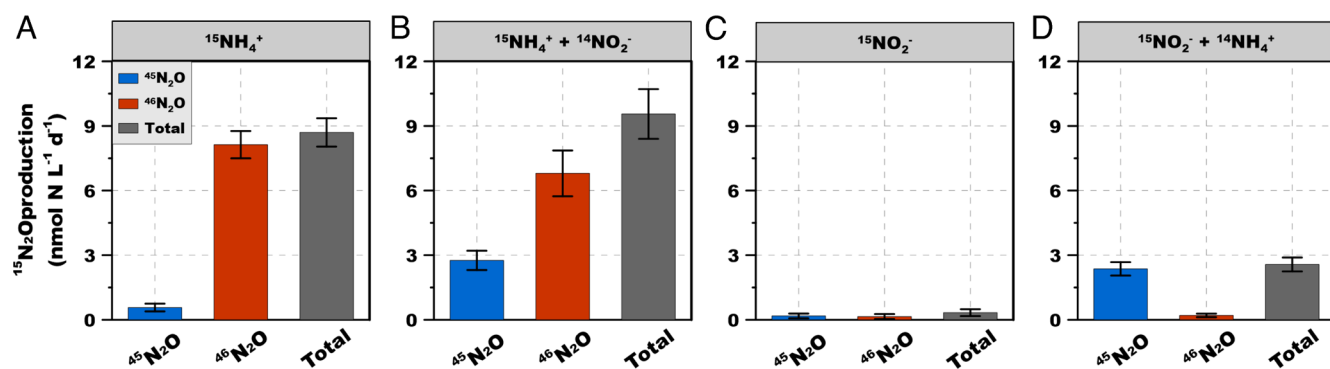


**Fig. 4.** Experiment 3.  $^{15}\text{N}$ - $\text{N}_2\text{O}$  production during  $^{15}\text{NH}_4^+$  and  $^{15}\text{NO}_2^-$  labeling incubations using viable cells. (A–D)  $^{15}\text{N}$  labeled  $\text{N}_2\text{O}$  production rate from  $^{15}\text{NH}_4^+$ ,  $^{15}\text{NH}_4^+ + ^{14}\text{NO}_2^-$ ,  $^{15}\text{NO}_2^-$ , and  $^{15}\text{NO}_2^- + ^{14}\text{NH}_4^+$  labeling incubations, respectively. Error bars represent SD from triplicate incubations. Total  $\text{N}_2\text{O}$  refers to total labeled  $\text{N}_2\text{O}$  ( $^{45}\text{N}_2\text{O} + ^{46}\text{N}_2\text{O}$ ). Approximately,  $6 \text{ nmol N L}^{-1} \text{ d}^{-1}$   $^{44}\text{N}_2\text{O}$  must have been produced in the  $^{15}\text{NO}_2^- + ^{14}\text{NH}_4^+$  incubation (D), but the amount of  $^{44}\text{N}_2\text{O}$  could not be determined in these experiments due to lack of sensitivity in small volume incubations.  $^{44}\text{N}_2\text{O}$  would not have been present in the other three experiments because in A all the  $\text{NH}_4^+$  was labeled; in B we have shown that  $\text{N}_2\text{O}$  cannot be formed from  $\text{NO}_2^-$  alone, and C all the  $\text{NO}_2^-$  was labeled.

which  $\text{NH}_2\text{OH}$  participates in  $\text{N}_2\text{O}$  production during ammonia oxidation (Experiment 4). Notably, here we used  $1 \mu\text{mol L}^{-1}$  of  $\text{NH}_2\text{OH}$  concentration, which was two orders of magnitude lower than previous studies that explored  $\text{N}_2\text{O}$  pathways by AOA (i.e.,  $200 \mu\text{mol L}^{-1}$ ) (13), thus closer to environmental concentrations but also ensuring the sensitivity of the assays to probe the potential mechanisms. Moreover, no discernible difference was observed for  $\text{NO}_2^-$  production with or without  $\text{NH}_2\text{OH}$  amendment, suggesting no detectable inhibition of  $1 \mu\text{mol L}^{-1}$  of  $\text{NH}_2\text{OH}$  on archaeal ammonia oxidation ( $P > 0.05$ ) (SI Appendix, Fig. S2).

$^{45}\text{N}_2\text{O}$  increased slowly but continuously over 12 h from tracer  $^{15}\text{NO}_2^-$  in viable cells, while no discernible  $^{46}\text{N}_2\text{O}$  accumulation was detected (Fig. 5A).  $^{14}\text{NH}_2\text{OH}$  added with  $^{15}\text{NO}_2^-$  stimulated  $^{45}\text{N}_2\text{O}$  production from  $^{15}\text{NO}_2^-$  in viable cells, indicating  $^{14}\text{NH}_2\text{OH}$  was directly involved in the reaction with  $^{15}\text{NO}_2^-$  to produce hybrid  $^{45}\text{N}_2\text{O}$  (Fig. 5B). In contrast,  $^{45}\text{N}_2\text{O}$  production nearly stopped after removing the cells by filtration. The fact that the viable cells produced more  $^{45}\text{N}_2\text{O}$  from the  $^{15}\text{NO}_2^-$  tracer than the filtrate indicates that cellular metabolism facilitated  $\text{N}_2\text{O}$  production from the hybrid pathway, and that abiotic formation rate of  $\text{N}_2\text{O}$  by  $\text{NO}_2^-$  and  $\text{NH}_2\text{OH}$  was low (Fig. 5C).

Much higher labeled  $\text{N}_2\text{O}$  production rates occurred in incubations supplemented with  $^{15}\text{NH}_2\text{OH}$  (Fig. 5D and E) than in incubations supplemented with either  $^{15}\text{NO}_2^-$  alone or  $^{15}\text{NO}_2^- + ^{14}\text{NH}_2\text{OH}$ , despite the concentration of  $^{15}\text{NO}_2^-$  ( $10 \mu\text{mol L}^{-1}$ ) being tenfold higher than  $^{15}\text{NH}_2\text{OH}$  ( $1 \mu\text{mol L}^{-1}$ ), demonstrating active involvement of  $\text{NH}_2\text{OH}$  in  $\text{N}_2\text{O}$  production. In the presence of viable cells, both  $^{45}\text{N}_2\text{O}$  and  $^{46}\text{N}_2\text{O}$  were produced

(Fig. 5D), while for the filtrate, only  $^{46}\text{N}_2\text{O}$  production was observed ( $^{45}\text{N}_2\text{O}$  accounted for  $<5\%$  of the total labeled  $\text{N}_2\text{O}$  production) (Fig. 5E). The comparable  $^{46}\text{N}_2\text{O}$  production between viable cell and filtrate groups indicated that  $^{46}\text{N}_2\text{O}$  was mainly produced via abiotic  $\text{NH}_2\text{OH}$  oxidation, and  $\text{NO}_2^-$  is not involved in that reaction. In contrast, viable cells are needed for the production of  $^{45}\text{N}_2\text{O}$  from  $^{15}\text{NH}_2\text{OH}$  and  $^{14}\text{NO}_2^-$ , suggesting the hybrid reaction may require enzymatic activity to produce  $\text{NO}$  from  $\text{NO}_2^-$ . Therefore, it appears that the ambient  $\text{NO}_2^-$  can enter the periplasmic space of the cell for the production of  $\text{NO}$  that is most likely catalyzed by a putative periplasmic copper-containing nitrite reductase (10, 11). These results indicate the central role of  $\text{NH}_2\text{OH}$  as a precursor of  $\text{N}_2\text{O}$  (pathways 1, 2, 3, and 4 in Fig. 1B). Moreover, the co-production of  $^{45}\text{N}_2\text{O}$  and  $^{46}\text{N}_2\text{O}$  from  $^{15}\text{NH}_2\text{OH}$  shows that hybrid  $\text{N}_2\text{O}$  formation and oxidation of  $\text{NH}_2\text{OH}$  both contributed to  $\text{N}_2\text{O}$  production in viable cells. Note that the high affinity for  $\text{NH}_4^+$  and the typical dependence of  $\text{N}_2\text{O}$  production rate on  $\text{NH}_4^+$  concentration (Experiment 1) implicate enzymatic control of  $\text{N}_2\text{O}$  production, even though the last step in both pathways (hybrid and  $\text{NH}_2\text{OH}$  oxidation) is abiotic.

Taking all the results with  $^{15}\text{N}$ -labeled substrates together, these findings demonstrate that N derived from both  $\text{NH}_4^+$  and  $\text{NO}_2^-$  is involved in  $\text{N}_2\text{O}$  production by AOA, but that  $\text{NH}_4^+$  is the major N source. Under the initial  $\text{NH}_4^+ : \text{NO}_2^-$  ratio of 1:1,  $\text{NH}_4^+$  accounts for  $\sim 85\%$  of N atoms to  $\text{N}_2\text{O}$ . Paired analysis of  $^{45}\text{N}_2\text{O} : ^{46}\text{N}_2\text{O}$  further implied that an additional  $\text{N}_2\text{O}$  formation pathway solely sourced from  $\text{NH}_4^+$  was required to explain the dominance

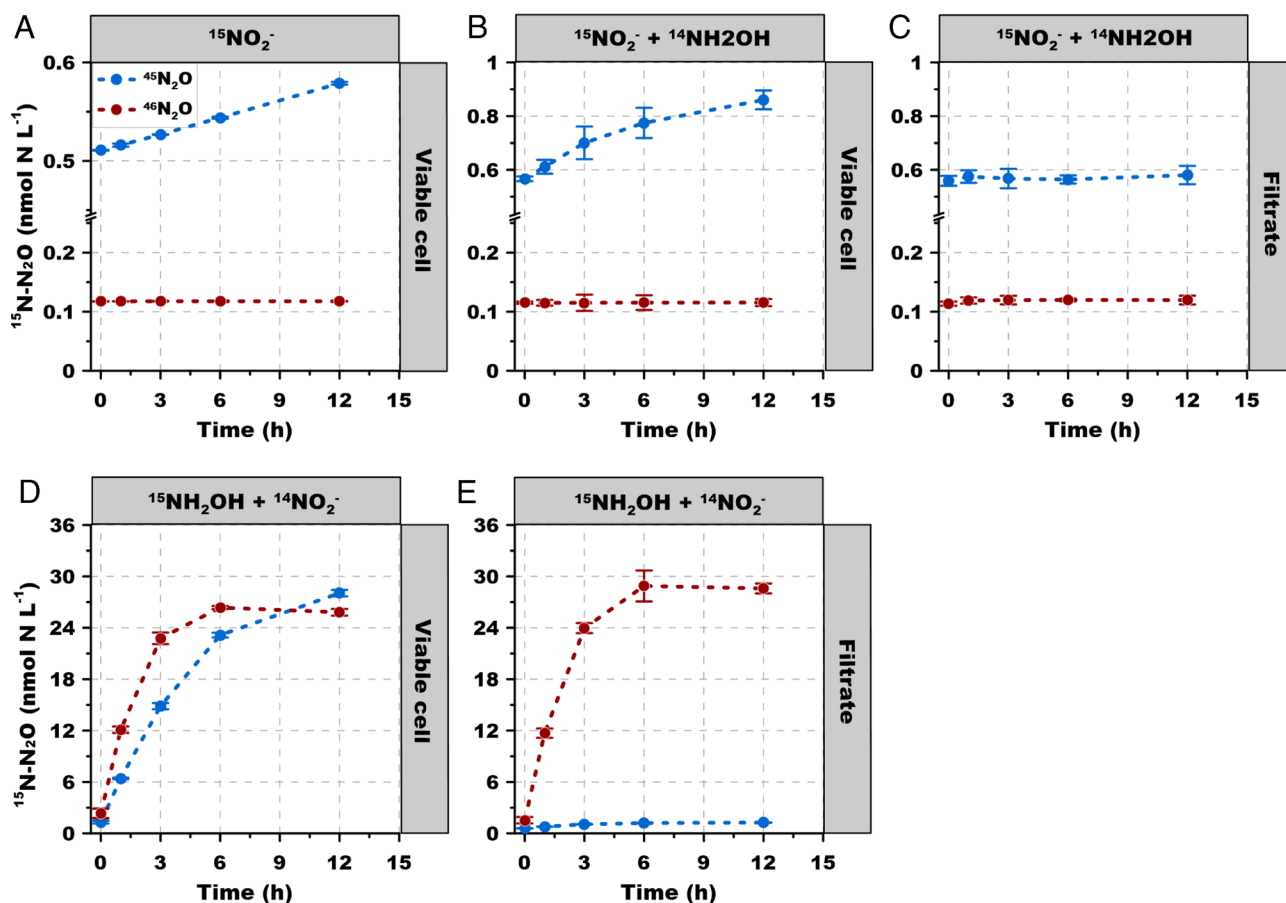


**Fig. 5.** Experiment 4.  $^{15}\text{N}-\text{N}_2\text{O}$  production from  $\text{NH}_2\text{OH}$ .  $^{15}\text{N}$  labeled  $\text{N}_2\text{O}$  production rate from (A) viable cells with  $^{15}\text{NO}_2^-$  tracer ( $10 \mu\text{mol L}^{-1}$ ); (B) viable cells with  $^{15}\text{NO}_2^-$  ( $10 \mu\text{mol L}^{-1}$ ) +  $^{14}\text{NH}_2\text{OH}$  ( $1 \mu\text{mol L}^{-1}$ ); (C) filtrate with  $^{15}\text{NO}_2^-$  ( $10 \mu\text{mol L}^{-1}$ ) +  $^{14}\text{NH}_2\text{OH}$  ( $1 \mu\text{mol L}^{-1}$ ); (D) viable cells with  $^{15}\text{NH}_2\text{OH}$  ( $1 \mu\text{mol L}^{-1}$ ) +  $^{14}\text{NO}_2^-$  ( $50 \mu\text{mol L}^{-1}$ ); (E) filtrate with  $^{15}\text{NH}_2\text{OH}$  ( $1 \mu\text{mol L}^{-1}$ ) +  $^{14}\text{NO}_2^-$  ( $50 \mu\text{mol L}^{-1}$ ). Error bars represent SD from triplicate samples.

of  $\text{NH}_4^+$  as the source of N atoms in  $\text{N}_2\text{O}$ . Thus, apart from the hybrid formation pathway,  $\text{NH}_2\text{OH}$  oxidation might be an important and previously overlooked pathway that contributes to archaeal  $\text{N}_2\text{O}$  production. However, it is difficult to discriminate all the associated pathways and to quantify the contributions of each process using N isotopes alone, because all N atoms in  $\text{N}_2\text{O}$  precursors could be directly or indirectly sourced from  $\text{NH}_4^+$ .

**Tracing the O in  $\text{N}_2\text{O}$ : Contributions of  $\text{H}_2\text{O}$ ,  $\text{O}_2$ , and  $\text{NO}_2^-$  as the Source of O in  $\text{N}_2\text{O}$ .**  $^{18}\text{O}$  leaves footprints in  $\text{N}_2\text{O}$  and  $\text{NO}_2^-$  that are independent of  $^{15}\text{N}$  and can thus provide further information on the pathways to  $\text{N}_2\text{O}$ . We developed a comprehensive set of  $^{18}\text{O}$ -labeling experiments to determine the source of O atoms in both  $\text{NO}_2^-$  and  $\text{N}_2\text{O}$ , and to quantify potential  $\text{N}_2\text{O}$  production pathways from  $\text{H}_2\text{O}$ ,  $\text{NO}_2^-$ , and  $\text{O}_2$  (Experiment 5). The isotopic enrichment of  $\delta^{18}\text{O}\text{-NO}_2^-$  showed an approximately linear increase over time in the 24 h abiotic O atom exchange experiment, i.e., from  $^{18}\text{O}\text{-H}_2\text{O}$  in the absence of viable cells (Fig. 6A). The measured values of  $\delta^{18}\text{O}\text{-NO}_2^-$  agreed well with the amount of  $\delta^{18}\text{O}\text{-NO}_2^-$  predicted using an exchange rate constant of 0.117 (33) under the experimental conditions (pH: 7.8; temperature: 30°C).

This correction for abiotic O atom exchange was applied to determine the  $\delta^{18}\text{O}$  of the produced  $\text{NO}_2^-$  in incubations with viable cells. O atoms from both  $\text{H}_2\text{O}$  and  $\text{O}_2$  were incorporated into  $\text{NO}_2^-$  during archaeal ammonia oxidation (and the amount of  $\delta^{18}\text{O}\text{-NO}_2^-$  was proportional to the amount of labeled substrate in both  $^{18}\text{O}\text{-H}_2\text{O}$  and  $^{18}\text{O}\text{-O}_2$  labeling incubations) (Fig. 6 B and C). The slope of  $\delta^{18}\text{O}\text{-NO}_2^-$  vs.  $\delta^{18}\text{O}\text{-H}_2\text{O}$  ( $63 \pm 3\%$ ) was significantly greater than the slope of  $\delta^{18}\text{O}\text{-NO}_2^-$  vs.  $\delta^{18}\text{O}\text{-O}_2$  ( $26 \pm 2\%$ )

( $P < 0.001$ ). The significantly higher contribution of  $\text{H}_2\text{O}$  than  $\text{O}_2$  to the O atoms in  $\text{NO}_2^-$  is consistent with the hypothesis that  $\text{NH}_2\text{OH}$  and  $\text{NO}$  act as co-substrates to produce two molecules of  $\text{NO}_2^-$ . Then one  $\text{NO}_2^-$  molecule is reduced back to  $\text{NO}$  and another O atom from  $\text{H}_2\text{O}$  is incorporated into  $\text{NO}_2^-$  (13). Alternatively, an intracellular O atom exchange could occur during  $\text{NO}_2^-$  production by AOA (SI Appendix, Text 2).

$\delta^{18}\text{O}$  of the produced  $\text{N}_2\text{O}$  increased with increasing  $\delta^{18}\text{O}\text{-H}_2\text{O}$ ,  $\delta^{18}\text{O}\text{-O}_2$  and  $\delta^{18}\text{O}\text{-NO}_2^-$ , indicating that O atoms from all three potential sources were incorporated into  $\text{N}_2\text{O}$  (Fig. 6 D–F) with different contributions. Interestingly, in contrast to the O atom source structure in  $\text{NO}_2^-$ ,  $\text{O}_2$  contributed the largest fraction of O atoms to  $\text{N}_2\text{O}$  ( $44 \pm 2\%$ ), followed by  $\text{NO}_2^-$  ( $30 \pm 3\%$ ) and  $\text{H}_2\text{O}$  ( $14 \pm 1\%$ ). Because the O atoms in  $\text{NH}_2\text{OH}$  are sourced from  $\text{O}_2$  and no further exchange occurs between  $\text{NH}_2\text{OH}$  and  $\text{H}_2\text{O}$  (34), the fact that  $\text{O}_2$  (via  $\text{NH}_2\text{OH}$ ) contributed most to O atoms in  $\text{N}_2\text{O}$  supports our finding of a substantial role for  $\text{NH}_2\text{OH}$  oxidation in producing  $\text{N}_2\text{O}$  (pathway 1 in Fig. 1B). The incorporation of O atoms from  $\text{NO}_2^-$  and  $\text{H}_2\text{O}$  into  $\text{N}_2\text{O}$  indicated internally produced and externally added (ambient)  $\text{NO}_2^-$  can both be involved in  $\text{N}_2\text{O}$  production. In the absence of known nitric oxide reductase catalyzing NO reduction to  $\text{N}_2\text{O}$  through nitrifier-denitrification, potential  $\text{N}_2\text{O}$  pathways associated with  $\text{NO}_2^-$  in marine AOA include abiotic  $\text{NO}_2^-$  reduction (chemo-denitrification-like) and hybrid formation. However, our  $^{15}\text{N}\text{-NO}_2^-$  labeling incubations showed that  $\text{NO}_2^-$  was involved in  $\text{N}_2\text{O}$  production only in the presence of  $\text{NH}_4^+$ , and  $\text{NO}_2^-$  alone did not contribute substantially to  $\text{N}_2\text{O}$  production (Fig. 4 C and D). Therefore, hybrid formation is the dominant pathway by which  $\text{NO}_2^-$  contributes to  $\text{N}_2\text{O}$  production.

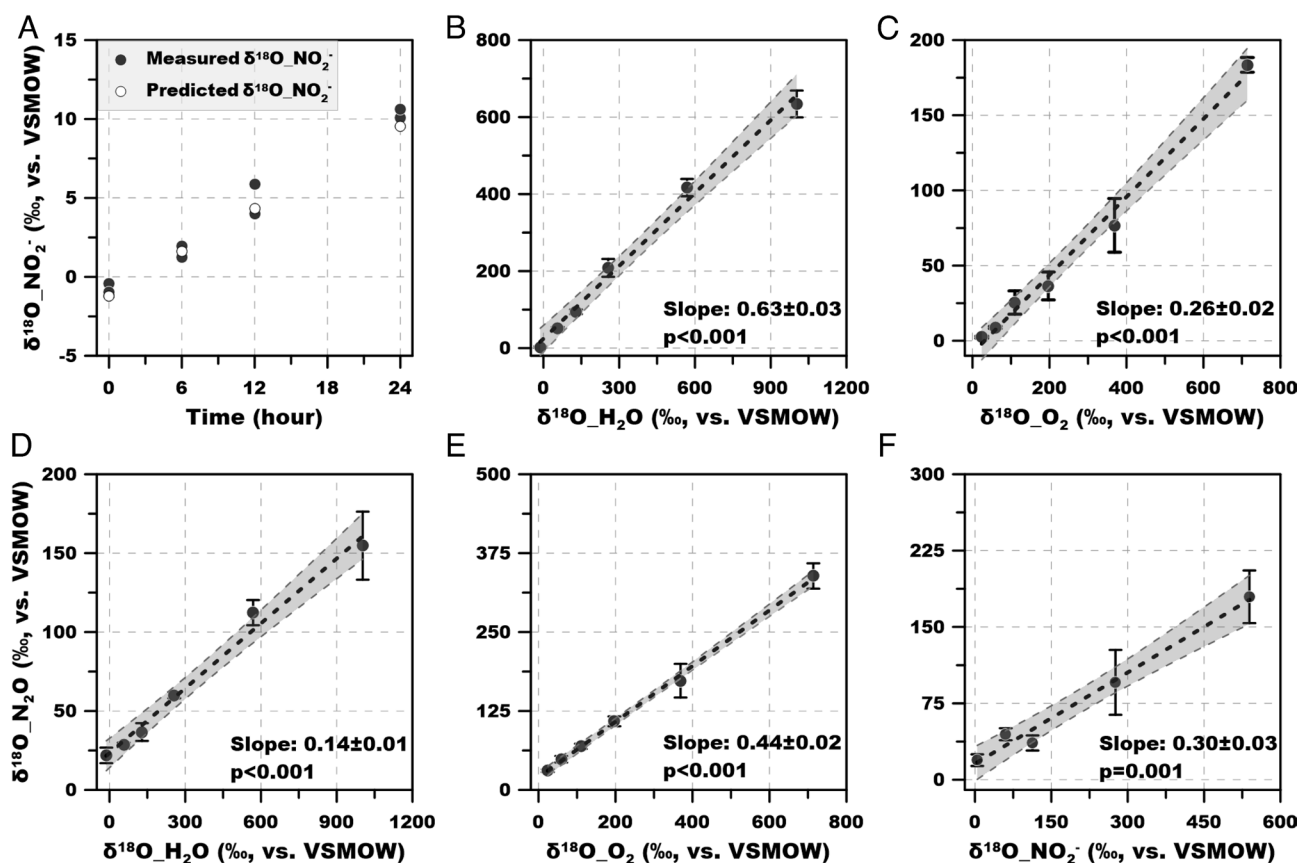


**Fig. 6.** Experiment 5.  $\delta^{18}\text{O}$  of the produced  $\text{NO}_2^-$  and  $\text{N}_2\text{O}$  during the 24 h  $^{18}\text{O}$ -labeling incubations. (A) Change of  $\delta^{18}\text{O}\text{-NO}_2^-$  due to abiotic O atom exchange. (B and C)  $\delta^{18}\text{O}$  of the produced  $\text{NO}_2^-$  in  $^{18}\text{O}\text{-H}_2\text{O}$  and  $^{18}\text{O}\text{-O}_2$  labeling experiments. (D–F)  $\delta^{18}\text{O}$  of the produced  $\text{N}_2\text{O}$  in  $^{18}\text{O}\text{-H}_2\text{O}$ ,  $^{18}\text{O}\text{-O}_2$ , and  $^{18}\text{O}\text{-NO}_2^-$  labeling experiments, respectively. Dashed lines denote the best linear regression, and gray shadow represents 95% CIs. Error bars represent SD from triplicate samples.

Moreover, the incorporation of O atoms from H<sub>2</sub>O and ambient NO<sub>2</sub><sup>-</sup> further revealed that during hybrid formation, O atoms in NO<sub>2</sub><sup>-</sup> or NO, rather than NH<sub>2</sub>OH, were retained in the N<sub>2</sub>O molecule. If the O atom was sourced from NH<sub>2</sub>OH during the hybrid process, all the O atoms should be contributed by O<sub>2</sub>. The incorporation of the O atom from ambient NO<sub>2</sub><sup>-</sup> into N<sub>2</sub>O also shows that at least some NO was produced via NO<sub>2</sub><sup>-</sup> reduction, as previously hypothesized (11, 14).

**Quantifying Multiple N<sub>2</sub>O Sources during Archaeal Ammonia Oxidation.** The dual-isotope labeling method enabled us to fully resolve multiple N<sub>2</sub>O production pathways in AOA. Combining results from <sup>15</sup>N and <sup>18</sup>O-labeling incubations (Experiments 3 to 5), we can quantitatively estimate the fractional contribution of the five potential N<sub>2</sub>O production pathways (Fig. 1B). NO<sub>2</sub><sup>-</sup> reduction (pathways 4 and 5) is an insignificant N<sub>2</sub>O source under aerobic growth conditions when both NH<sub>4</sub><sup>+</sup> and NO<sub>2</sub><sup>-</sup> are present in equimolar amounts (Fig. 4). NH<sub>2</sub>OH is revealed as the main contributor to N<sub>2</sub>O production (Fig. 5) via both hybrid pathway and NH<sub>2</sub>OH oxidation. In NH<sub>2</sub>OH oxidation (pathway 1), 100% of O atoms in N<sub>2</sub>O were sourced from O<sub>2</sub>, while in hybrid formation (pathways 2 and 3), the O atom was derived from NO<sub>2</sub><sup>-</sup> via reduction to NO. The NH<sub>2</sub>OH involved in hybrid N<sub>2</sub>O formation contributed an N atom but not the O atom. There were two sources of NO<sub>2</sub><sup>-</sup>: the original ambient NO<sub>2</sub><sup>-</sup> (100% of O atoms were sourced from ambient NO<sub>2</sub><sup>-</sup>) and the NO<sub>2</sub><sup>-</sup> newly produced from ammonia oxidation (63% of O atoms from H<sub>2</sub>O and 26% from O<sub>2</sub>) (Fig. 6). Under these conditions, we calculated the following contributions to O atoms in N<sub>2</sub>O: 38.2% from NH<sub>2</sub>OH oxidation (pathway 1), 59.8% from the hybrid source (22.2% by pathway 2 and 37.6% by pathway 3), and 2.1% from NO<sub>2</sub><sup>-</sup> reduction (pathways 4 and 5) (Fig. 1C). This combination best fits the observed results that 14% of O atoms in N<sub>2</sub>O were from H<sub>2</sub>O and 44% of O atoms were from O<sub>2</sub> under our experimental conditions. Although the fractional contribution of the pathways might vary with various substrate concentrations (i.e., different NH<sub>4</sub><sup>+</sup>:NO<sub>2</sub><sup>-</sup> ratios), the comprehensive <sup>15</sup>N-<sup>18</sup>O dual-isotope labeling technique developed here provides a novel avenue to disentangle and quantify the relative contribution of multiple pathways to N<sub>2</sub>O production in both lab and field studies.

Archaeal ammonia oxidation is the primary source of marine N<sub>2</sub>O, yet the mechanistic understanding of archaeal N<sub>2</sub>O production remains elusive. We present the first study determining the kinetics of archaeal N<sub>2</sub>O production and provide strong evidence of the capability of marine AOA in producing N<sub>2</sub>O at trace levels of NH<sub>4</sub><sup>+</sup>, supporting their dominant role in contributing to N<sub>2</sub>O production in the ocean. We further show a direct control of NH<sub>4</sub><sup>+</sup> and NO<sub>2</sub><sup>-</sup> concentrations on the sources of N<sub>2</sub>O, providing new insights into understanding the varying isotope composition of N<sub>2</sub>O in the ocean. The increased incorporation of N and O atoms from NO<sub>2</sub><sup>-</sup> into N<sub>2</sub>O by marine AOA at low NH<sub>4</sub><sup>+</sup>:NO<sub>2</sub><sup>-</sup> ratios suggests a new mechanism for interpreting the ubiquitous N<sub>2</sub>O isotope minimum without the need to invoke nitrifier-denitrification by AOB, which are rarely detected in the oligotrophic open ocean. Our comprehensive dual <sup>15</sup>N-<sup>18</sup>O-labeling techniques identify a substantial contribution of NH<sub>2</sub>OH oxidation to archaeal N<sub>2</sub>O production that was previously not recognized. These explicit descriptions of the N<sub>2</sub>O production pathways and kinetics in AOA should improve our understanding of marine N<sub>2</sub>O production, and the multiple N and O atom sources of N<sub>2</sub>O identified here should inform biogeochemical models that aim to resolve the marine nitrogen cycle and constrain the air-sea N<sub>2</sub>O flux. Moreover, our dual-isotope labeling technique could be applied

in combination with manipulative experiments, such as temperature, pH, and dissolved oxygen (DO), to explore rates and pathways of archaeal N<sub>2</sub>O production in response to ocean warming, acidification and deoxygenation.

## Materials and Methods

**SCM1 Cultivation and Isotope Labeling Incubation.** *N. maritimus* strain SCM1 was cultured in 4-(2-hydroxyethyl)-1-piperazineethanesulfonic acid (HEPES) buffered Synthetic Crenarchaeota Medium (SCM) (pH: ~7.8) at 30 °C in the dark following Qin et al. (2014) (35). Six sets of incubations were carried out (SI Appendix, Table S1). The SCM1 cells were grown and maintained in 2-L bottles containing 600 mL SCM for the preservative test and experiments 3 to 5 and were grown in 100-mL bottles containing 40 mL SCM for experiments 1 to 2. The medium contains FeNaEDTA and other trace metals including, Cu, Ni, Zn, and Co. The approximate concentrations of the trace metals can be found in Amin et al. (2013) (36). The medium was supplemented with NH<sub>4</sub>Cl at different initial concentrations for each of the experiments: Initial concentrations were 1,000 μmol L<sup>-1</sup> in the preservative test experiment, 500 μmol L<sup>-1</sup> in experiments 3 and 5, 200 μmol L<sup>-1</sup> in experiment 1 and 2, and 100 μmol L<sup>-1</sup> in experiments 4. Growth was monitored both by measuring NO<sub>2</sub><sup>-</sup> concentration and NH<sub>4</sub><sup>+</sup> consumption and by performing cell counts using flow cytometry (Accuri C6, BD Biosciences). After determining the best strategy for terminating the incubation to preserve the concentration and isotopic content of analytes (Preservative Test), the five experimental incubations were carried out to 1) test the kinetic response of N<sub>2</sub>O production during SCM1 ammonia oxidation; 2) examine the impact of NH<sub>4</sub><sup>+</sup>:NO<sub>2</sub><sup>-</sup> substrate ratio on the pathways and composition of N atoms in N<sub>2</sub>O; 3) track N atom sources through <sup>15</sup>N labeling experiments; 4) test the contribution of ambient NH<sub>2</sub>OH to N<sub>2</sub>O production; and 5) track O atom sources through multiple <sup>18</sup>O-labeling experiments. All labeling incubation experiments were performed using mid- to late-exponential phase cultures.

**Preservative test.** A total of ~1.0 L of culture was collected and aliquoted into two groups in the mid-exponential phase: 1) viable cells and 2) killed control (autoclaved at 120°C for 30 min and cooled overnight). In each group, each <sup>15</sup>N tracer (<sup>15</sup>NH<sub>4</sub><sup>+</sup> and <sup>15</sup>NO<sub>2</sub><sup>-</sup>, 99% <sup>15</sup>N, Cambridge, United States) was added to separate bottles to a concentration of 50 μmol L<sup>-1</sup>. For the viable cells, one additional treatment (100 μmol L<sup>-1</sup> of <sup>15</sup>NO<sub>3</sub><sup>-</sup>, 98% <sup>15</sup>N, Cambridge, United States) was performed. After tracer addition, 10 mL of sample was dispensed into triplicate 20-mL serum bottles and sealed with 20-mm butyl stoppers and aluminum crimp seals (Wheaton, United States). Two preservatives (20 μL of saturated HgCl<sub>2</sub> and 500 μL of 10 mol L<sup>-1</sup> of NaOH) were used to compare the effect of preservatives on terminating biological activity and archaeal N<sub>2</sub>O production. For the viable cells, the incubations were performed at 30°C in the dark and terminated at 0 and 24 h. For the autoclaved samples, the preservatives were added only at 0 h. All incubations were performed in triplicate. Our results showed that HgCl<sub>2</sub> induces artifacts of N<sub>2</sub>O production from pathways involving NO<sub>2</sub><sup>-</sup>. Such artifacts are negligible when using NaOH as a preservative (SI Appendix, Fig. S3 and Text 3). Thus, NaOH was chosen as the preservative for all further experiments.

**Experiment 1: Kinetic test.** When all amended NH<sub>4</sub><sup>+</sup> (200 μmol L<sup>-1</sup>) was completely consumed (i.e., below the substrate threshold of SCM1, ~10 nmol L<sup>-1</sup> NH<sub>4</sub><sup>+</sup>), 1% inoculum was transferred into NH<sub>4</sub><sup>+</sup> free fresh medium supplemented with labeled tracers. The initial cell abundance was around 1.39 × 10<sup>5</sup> cells mL<sup>-1</sup>, which is comparable to AOA cell abundance in the ocean, and initial carry over <sup>14</sup>NO<sub>2</sub><sup>-</sup> concentration was ~2 μmol L<sup>-1</sup>. A total of eight <sup>15</sup>NH<sub>4</sub><sup>+</sup> concentrations (0.1, 0.5, 1, 1.5, 2, 5, 8, 10 μmol L<sup>-1</sup>) were used for the kinetic test. Immediately after tracer amendment, 50 mL aliquots of sample were dispensed into 60-mL serum bottles and sealed with 20-mm butyl stoppers and aluminum crimp seals (Wheaton, United States). The incubation was performed at 30°C in the dark. Depending on the initial <sup>15</sup>NH<sub>4</sub><sup>+</sup> concentration, the incubation was terminated at 0 h, ~2 h (0.1 μmol L<sup>-1</sup>), ~6 h (0.5 μmol L<sup>-1</sup>), and ~12 h (>0.5 μmol L<sup>-1</sup>) by adding 2.5 mL of 10 mol L<sup>-1</sup> of NaOH. A third time point (~24 h) was also applied for all treatments. However, the third time point was only used for rate calculation in the high NH<sub>4</sub><sup>+</sup> treatments (>1.5 μmol L<sup>-1</sup>) because the substrate

was nearly completely consumed or exhausted before 24 h in those low substrate treatments. The incubations were carried out in triplicates at each time point.

**Experiment 2: Substrate ratio experiment.** When  $100 \mu\text{mol L}^{-1}$  of  $\text{NH}_4^+$  was consumed, 1% inoculum was transferred into  $\text{NH}_4^+$  free medium. The initial cell abundance was around  $6.2 \times 10^4$  cells  $\text{mL}^{-1}$ . Three  $\text{NH}_4^+ : \text{NO}_2^-$  ratios were achieved by adding different amounts of  $^{15}\text{NH}_4^+$  and  $^{14}\text{NO}_2^-$  (10 and  $1 \mu\text{mol L}^{-1}$  of  $\text{NH}_4^+$  and  $\text{NO}_2^-$ , 5 and  $5 \mu\text{mol L}^{-1}$  of  $\text{NH}_4^+$  and  $\text{NO}_2^-$ , and 1.5 and  $15 \mu\text{mol L}^{-1}$  of  $\text{NH}_4^+$  and  $\text{NO}_2^-$ , respectively). Immediately after tracer amendment, 40 mL aliquots of sample were dispensed into 60-mL serum bottles and sealed with 20-mm butyl stoppers and aluminum crimp seals (Wheaton, United States). The incubation was performed at  $30^\circ\text{C}$  in the dark and terminated by adding  $2 \text{ mL}$  of  $10 \text{ mol L}^{-1}$  of NaOH at 0, 6 and 24 h with triplicates at each time point.

**Experiment 3: Source of N atoms in  $\text{N}_2\text{O}$ .** A total of  $\sim 4 \text{ L}$  of culture was harvested by gentle filtration onto two  $0.2 \mu\text{m}$  pore size Sterivex filters (Millipore). Immediately after the filtration, the filters were flushed using 2-L fresh substrate-free medium to collect the cells and to remove the high background  $\text{NH}_4^+$  ( $\sim 210 \mu\text{mol L}^{-1}$ ) and  $\text{NO}_2^-$  ( $\sim 330 \mu\text{mol L}^{-1}$ ). The cell densities before (4 L original culture) and after the filtration (resuspended in 2 L medium) were  $1.15 \times 10^7$  and  $2.10 \times 10^7$  cells  $\text{mL}^{-1}$ , respectively, demonstrating a good recovery efficiency ( $\sim 60\%$ ) of the pre-concentration process. The measured ammonia oxidation rate of the washed cells ( $\sim 16 \mu\text{mol N L}^{-1} \text{ d}^{-1}$ ) was lower than the rate of unwashed cells measured on the same day ( $\sim 84 \mu\text{mol N L}^{-1} \text{ d}^{-1}$ ). This reduced oxidation rate indicates that the manipulation process caused physiological stress on the SCM1 cells and resulted in decreased cellular activity. Nevertheless, the activity of the washed cells was high enough to allow precise measurement of rates of ammonia oxidation and  $\text{N}_2\text{O}$  production in the experiments. The recovered cells were aliquoted into eight acid washed 250-mL PC bottles (Nalgene) and for four groups of tracers ( $^{15}\text{NH}_4^+$ ,  $^{15}\text{NH}_4^+ + ^{14}\text{NO}_2^-$ ,  $^{15}\text{NO}_2^-$ ,  $^{15}\text{NO}_2^- + ^{14}\text{NH}_4^+$ ). Immediately after tracer amendment, 10 mL aliquots of sample were dispensed into 20-mL serum bottles and sealed with 20-mm butyl stopper and aluminum crimp seals (Wheaton, United States). The incubation was performed at  $30^\circ\text{C}$  in the dark and terminated by adding  $500 \mu\text{L}$  of  $10 \text{ mol L}^{-1}$  of NaOH at 0 and 24 h with triplicates at each time point.

**Experiment 4: Role of  $\text{NH}_2\text{OH}$  in  $\text{N}_2\text{O}$  production.** Around 1 L of culture was aliquoted into five groups when  $50 \mu\text{mol L}^{-1}$  of  $\text{NH}_4^+$  had been oxidized: 1) viable cells amended with  $^{15}\text{NO}_2^-$  ( $10 \mu\text{mol L}^{-1}$ ); 2) viable cells amended with  $^{15}\text{NO}_2^-$  ( $10 \mu\text{mol L}^{-1}$ ) +  $^{14}\text{NH}_2\text{OH}$  ( $1 \mu\text{mol L}^{-1}$ ); 3) filtrate (through  $0.2 \mu\text{m}$  PES filter) amended with  $^{15}\text{NO}_2^-$  ( $10 \mu\text{mol L}^{-1}$ ) +  $^{14}\text{NH}_2\text{OH}$  ( $1 \mu\text{mol L}^{-1}$ ); 4) viable cells amended with  $^{15}\text{NH}_2\text{OH}$  ( $1 \mu\text{mol L}^{-1}$ ); and 5) filtrate (through  $0.2 \mu\text{m}$  PES filter) amended with  $^{15}\text{NH}_2\text{OH}$  ( $1 \mu\text{mol L}^{-1}$ ). After tracer amendment, 10 mL aliquots of sample were dispensed into 20-mL serum bottles and sealed with 20-mm butyl stoppers and aluminum crimp seals (Wheaton, United States). Time-course incubation (0, 1, 3, 6, 12 h) was carried out for all the groups, and the incubation was performed at  $30^\circ\text{C}$  in the dark with triplicates and terminated by adding  $500 \mu\text{L}$  of  $10 \text{ mol L}^{-1}$  of NaOH at each time point.

**Experiment 5: Source of O atoms in  $\text{N}_2\text{O}$ .** A total of  $\sim 7.2 \text{ L}$  of culture was harvested by gentle filtration onto two  $0.2 \mu\text{m}$  pore size Sterivex filters (Millipore). Immediately after the filtration, the filters were back flushed using 2.5 L fresh substrate-free medium to collect the cells and to remove the high background  $\text{NH}_4^+$  and  $\text{NO}_2^-$ . Three groups of tracers ( $\text{H}_2^{18}\text{O}$ ,  $^{18}\text{O}_2$  and  $\text{N}^{18}\text{O}_2^-$ ) were used to track the source of the O atom. For the  $^{18}\text{O}$ - $\text{H}_2\text{O}$  labeling experiment, a range of  $\delta^{18}\text{O}$ - $\text{H}_2\text{O}$  tracer amendments ( $-13$  to  $1003\%$ ) were made by adding  $0.2 \text{ mL}$  of  $^{18}\text{O}$ - $\text{H}_2\text{O}$  stocks with different  $^{18}\text{O}$  enrichment into the samples ( $^{18}\text{O}$ - $\text{H}_2\text{O}$  stocks were made by mixing the  $\text{H}_2^{18}\text{O}$  ( $99\% \text{ } ^{18}\text{O}$ , Sigma-Aldrich, United States) with distilled deionized  $\text{H}_2\text{O}$ ). Similarly, six levels of  $\delta^{18}\text{O}$ - $\text{O}_2$  ( $24$  to  $714\%$ ) were made by adding  $0.2 \text{ mL}$  of  $^{18}\text{O}$ - $\text{O}_2$  stocks with different  $^{18}\text{O}$  enrichment ( $^{18}\text{O}$ - $\text{O}_2$  stocks were made by mixing the  $^{18}\text{O}_2$  ( $99\% \text{ } ^{18}\text{O}$ , Sigma-Aldrich, United States) with He) into the samples. For the  $^{18}\text{O}$ - $\text{NO}_2^-$  labeling experiment, five levels of  $^{18}\text{O}$ - $\text{NO}_2^-$  ( $4$  to  $539\%$ ) were made by using the O atom exchange between  $\text{NO}_2^-$  and  $\text{H}_2^{18}\text{O}$ . In each treatment,  $20 \text{ mL}$  of sample was dispensed into 60-mL serum bottles and sealed with 20-mm butyl stoppers and aluminum crimp seals (Wheaton, United States). The  $^{18}\text{O}$ -labeled substrates were injected into the serum bottles. Both the  $\text{NH}_4^+$  and  $\text{NO}_2^-$  were set at  $20 \mu\text{mol L}^{-1}$  in each incubation. For  $^{18}\text{O}_2$  labeled incubations, after  $^{18}\text{O}_2$  injection, the bottles were shaken at  $\sim 120 \text{ rpm}$  for 15 min to equilibrate the  $^{18}\text{O}_2$  with the dissolved oxygen (DO) in water. The

incubation was performed at  $30^\circ\text{C}$  in the dark and terminated by adding  $1 \text{ mL}$  of  $10 \text{ mol L}^{-1}$  NaOH. A time-course (0, 6, 12, 24 h) incubation was performed in selected tracer treatments ( $\delta^{18}\text{O}$ - $\text{H}_2\text{O}$  of  $129\%$ ;  $\delta^{18}\text{O}$ - $\text{O}_2$  of  $110\%$ ;  $\delta^{18}\text{O}$ - $\text{NO}_2^-$  of  $276\%$ ), and the remaining treatments were terminated at 0 and 24 h; all experiments were performed in triplicates at each time point. An additional set of experiments was performed to examine the rate of abiotic O atom exchange between  $\text{NO}_2^-$  and  $\text{H}_2\text{O}$ . Briefly,  $\text{NH}_4^+$  and  $\text{NO}_2^-$  were added into  $\sim 10 \text{ mL}$  of fresh medium to a concentration of  $20 \mu\text{mol L}^{-1}$ , and  $\sim 0.1 \text{ mL}$  of  $^{18}\text{O}$ - $\text{H}_2\text{O}$  stock was added to get  $\delta^{18}\text{O}$ - $\text{H}_2\text{O}$  of  $\sim 76\%$ . The incubation was performed at  $30^\circ\text{C}$  in the dark and terminated by adding  $500 \mu\text{L}$  of  $10 \text{ mol L}^{-1}$  of NaOH at 0, 6, 12, and 24 h with duplicates at each time point.

**Sample Analysis.** The samples for  $\text{NH}_4^+$  and  $\text{NO}_2^-$  concentration measurement were stored at  $-20^\circ\text{C}$  until analysis. The concentration of  $\text{NH}_4^+$  and  $\text{NO}_2^-$  was measured by colorimetric methods with an AA3 nutrient analyzer or a spectrophotometer. The detection limit for  $\text{NH}_4^+$  and  $\text{NO}_2^-$  was 0.5 and  $0.03 \mu\text{mol L}^{-1}$ , and the analytical precision was better than  $\pm 3\%$  and  $\pm 1\%$ , respectively (37).

The  $\text{N}_2\text{O}$  samples were stored at  $4^\circ\text{C}$  after incubation. For the preservative test and experiments 3 and 4, before measurements,  $1.5 \text{ nmol}$  of  $\text{N}_2\text{O}$  of known isotope composition ( $\delta^{15}\text{N} = -3.2 \pm 0.1\%$  relative to air  $\text{N}_2$ ,  $\delta^{18}\text{O} = 36.6 \pm 0.1\%$  relative to Vienna Standard Mean Ocean Water) was introduced into each serum bottle to provide enough mass for isotopic analysis. For experiments 1, 2, and 5, the samples were measured directly without  $\text{N}_2\text{O}$  carrier addition. Concentration and isotopes of  $\text{N}_2\text{O}$  were measured using a modified Gas Chromatograph-Isotope Ratio Mass Spectrometer (GC-IRMS) (38). Briefly, two needles were used for He pressurization and  $\text{N}_2\text{O}$  purging. For the 20-mL bottles, sample was purged for 6.7 min at a flow rate of  $40 \text{ mL min}^{-1}$ , and for 60-mL bottles, the purge time was 30 min. The extracted gases were passed through an ethanol trap with dry ice and a chemical trap filled with magnesium perchlorate and Ascarite to remove  $\text{H}_2\text{O}$  and  $\text{CO}_2$ .  $\text{N}_2\text{O}$  was trapped by liquid nitrogen twice for purification and concentration and then injected into the GC-IRMS with He as carrier gas.  $\text{N}_2\text{O}$  mass was determined by ion peak area [m/z of 44, 45, 46] with standard gases of 199.6, 501.0, and 1,000.2 ppmv  $\text{N}_2\text{O}/\text{He}$ , which were run at ten sample intervals. The precision of this method for  $\text{N}_2\text{O}$  mass measurement was estimated to be better than  $\pm 3\%$ .  $\delta^{15}\text{N}$  and  $\delta^{18}\text{O}$  were calibrated against two reference tanks (R1: 199.6 ppmv  $\text{N}_2\text{O}/\text{He}$ ,  $\delta^{15}\text{N} = -3.2 \pm 0.1\%$ ,  $\delta^{18}\text{O} = 36.6 \pm 0.1\%$ ; R2: 501.0 ppmv  $\text{N}_2\text{O}/\text{He}$ ,  $\delta^{15}\text{N} = -1.6 \pm 0.1\%$ ,  $\delta^{18}\text{O} = 36.6 \pm 0.3\%$ ). The precision of  $\delta^{15}\text{N}$  and  $\delta^{18}\text{O}$  measurements with 2 nmol  $\text{N}_2\text{O}$  reference gas was better than 0.3‰ and 0.4‰, respectively ( $n = 20$ ) (30). All the samples were measured within 2 wk after the incubations.

After  $\text{N}_2\text{O}$  measurement, the samples were stored at  $4^\circ\text{C}$  before further analysis.  $\delta^{15}\text{N}$  and  $\delta^{18}\text{O}$  of  $\text{NO}_2^-$  were determined using the bacterial denitrifier method (39, 40) using a Thermo Finnigan Gasbench system with cryogenic extraction and purification system interfaced to a Delta V<sup>PLUS</sup> isotopic ratio mass spectrometer. Briefly,  $\sim 5$  to  $10 \text{ nmol}$  of  $\text{NO}_2^-$  was quantitatively converted to  $\text{N}_2\text{O}$  using the bacterial strain *Pseudomonas aureofaciens*. The produced  $\text{N}_2\text{O}$  was then introduced to the GC-IRMS through an online  $\text{N}_2\text{O}$  cryogenic extraction and purification system.  $\delta^{15}\text{N}$  of  $\text{NO}_2^-$  values were calibrated against  $\text{NO}_3^-$  isotope standards USGS 34, IAEA N3, and USGS 32;  $\delta^{18}\text{O}$  of  $\text{NO}_2^-$  values were calibrated against  $\text{NO}_3^-$  isotope standards USGS 34, IAEA N3 and USGS 35. The standards were run before, after, and at ten sample intervals. Because of the different branching effect during  $\text{NO}_3^-$  and  $\text{NO}_2^-$  reduction by *P. aureofaciens* (i.e., 38‰ vs. 12‰), the  $\delta^{18}\text{O}$  of  $\text{NO}_2^-$  was further calibrated by taking account of the branching effect between  $\text{NO}_3^-$  and  $\text{NO}_2^-$  (26‰) (41). Accuracy (pooled SD) was better than  $\pm 0.2\%$  for  $\delta^{15}\text{N}$  and  $\pm 0.4\%$  for  $\delta^{18}\text{O}$  according to analyses of these standards with an injection of a similar amount of  $\text{NO}_3^-$ . Quality control was also conducted by analyzing laboratory working reference material (3,000 m deep sea water from the South China Sea).

$\delta^{18}\text{O}$  of  $\text{H}_2\text{O}$  was measured following McIlvin and Casciotti (2006) (42) using the full exchange of O atom between  $\text{H}_2\text{O}$  and  $\text{NO}_2^-$  under acidic conditions (pH: 6) at room temperature ( $\sim 25^\circ\text{C}$ ) for 2 wk.  $\delta^{18}\text{O}$  of  $\text{NO}_2^-$  was measured as described above, and  $\delta^{18}\text{O}$  of  $\text{H}_2\text{O}$  was calculated based on the isotope effect of 13‰ between the O atom exchange at room temperature (33).

$\delta^{18}\text{O}$  of  $\text{O}_2$  was not measured directly. The  $\delta^{18}\text{O}$  of the  $^{18}\text{O}_2$  tracer was calculated from the mixing ratio of air (assuming  $\delta^{18}\text{O}$  air  $\text{O}_2$  is 24‰) and  $^{18}\text{O}_2$  tracer. Briefly, during our incubation, the DO concentration in the medium was near equilibration with air ( $\sim 244 \mu\text{mol L}^{-1}$ ); thus, a total of  $\sim 348 \mu\text{mol}$  of  $\text{O}_2$  was present in the bottle (20 mL of medium and 40 mL of air in the headspace). During the  $^{18}\text{O}$ - $\text{O}_2$  labeling incubation, 0 to  $12 \mu\text{L}$  of  $^{18}\text{O}_2$  gas was introduced into



the headspace and was then fully equilibrated with the water to attain different enrichments of  $^{18}\text{O}$  in the incubation, and the  $\delta^{18}\text{O}$  was then calculated from the  $^{18}\text{O}/^{16}\text{O}$  after tracer addition.

**Calculations.** Rate of labeled  $\text{N}_2\text{O}$  production from the  $^{15}\text{N}$ -labeled substrate was calculated based on the accumulation of  $^{45}\text{N}_2\text{O}$  (single labeled) and  $^{46}\text{N}_2\text{O}$  (double labeled) during the incubation. Total labeled  $\text{N}_2\text{O}$  production rate was defined as the  $^{15}\text{N}$  from both  $^{45}\text{N}_2\text{O}$  and  $^{46}\text{N}_2\text{O}$  (Eq. 1).  $^{15}\text{NH}_4^+$  oxidation rate was calculated from the increase of  $^{15}\text{NO}_2^-$ .

$$^{15}\text{N} - \text{N}_2\text{O} = ^{45}\text{N}_2\text{O} + 2 \times ^{46}\text{N}_2\text{O}, \quad [1]$$

where the total  $^{15}\text{N}$ - $\text{N}_2\text{O}$  includes  $^{15}\text{N}$  atom from  $^{45}\text{N}_2\text{O}$  (one  $^{15}\text{N}$  atom) and  $^{46}\text{N}_2\text{O}$  (two  $^{15}\text{N}$  atoms in each molecule).

$\delta^{18}\text{O}$  of the produced  $\text{N}_2\text{O}$  during the incubation was calculated using a two-endmember mixing model (Eq. 2) (43).

$$\delta^{18}\text{O} - \text{N}_2\text{O}_p = \frac{M_{t24} \times \delta^{18}\text{O}_{\text{N}_2\text{O}_{t24}} - M_{t0} \times \delta^{18}\text{O}_{\text{N}_2\text{O}_{t0}}}{M_{t24} - M_{t0}}, \quad [2]$$

where  $\delta^{18}\text{O}$ - $\text{N}_2\text{O}_p$ ,  $\delta^{18}\text{O}$ - $\text{N}_2\text{O}_{t24}$ , and  $\delta^{18}\text{O}$ - $\text{N}_2\text{O}_{t0}$  denote the  $\delta^{18}\text{O}$ - $\text{N}_2\text{O}$  value of the net produced  $\text{N}_2\text{O}$  during the  $^{18}\text{O}$ -labeling incubation,  $\delta^{18}\text{O}$ - $\text{N}_2\text{O}$  at the end and beginning of incubation, respectively.  $M_{t24}$  and  $M_{t0}$  denote the measured  $\text{N}_2\text{O}$  mass at the end and beginning of incubation, respectively.

$\delta^{18}\text{O}$  of the produced  $\text{NO}_2^-$  during the  $^{18}\text{O}$ - $\text{H}_2\text{O}$  and  $^{18}\text{O}$ - $\text{O}_2$  incubations was calculated using Eq. 2 after calibrating the abiotic O atom exchange between  $\text{NO}_2^-$  and  $\text{H}_2\text{O}$  (9, 33). Briefly, the abiotic O atom exchange rate was derived from the time-course experiment using cell-free medium, which was then used to calibrate the contribution of abiotic O atom exchange during our incubation (Eq. 3). The difference between the measured  $^{18}\text{O}$ - $\text{NO}_2^-$  and the predicted  $^{18}\text{O}$ - $\text{NO}_2^-$  by abiotic

exchange was then used to calculate the  $\delta^{18}\text{O}$  of newly produced  $\text{NO}_2^-$  during the incubation. The slopes of the newly produced  $\delta^{18}\text{O}$ - $\text{NO}_2^-$  and  $\delta^{18}\text{O}$ - $\text{N}_2\text{O}$  against  $\delta^{18}\text{O}$  of different substrates ( $\text{H}_2\text{O}$ ,  $\text{O}_2$ ,  $\text{NO}_2^-$ ) were identified as the fraction contribution of O atom from various substrates to the  $\text{NO}_2^-$  and  $\text{N}_2\text{O}$  (9, 33).

$$\delta^{18}\text{O}_{\text{NO}_2^-\text{abio}} = (\delta^{18}\text{O}_{\text{NO}_2^-\text{t0}} - \delta^{18}\text{O}_{\text{NO}_2^-\text{t24}}) \times \exp(-k \times t) + \delta^{18}\text{O}_{\text{NO}_2^-\text{t24}}, \quad [3]$$

where  $\delta^{18}\text{O}$ - $\text{NO}_2^-\text{abio}$ ,  $\delta^{18}\text{O}$ - $\text{NO}_2^-\text{t0}$ , and  $\delta^{18}\text{O}$ - $\text{NO}_2^-\text{t24}$  are  $\delta^{18}\text{O}$  value of  $\text{NO}_2^-$  at the end, beginning, and the equilibrated  $\text{NO}_2^-$  with  $\text{H}_2\text{O}$  due to abiotic O exchange.  $t$  is the incubation length in hours and  $k$  is the rate constant.

**Data, Materials, and Software Availability.** All data needed to evaluate the conclusions in the paper are deposited in Zenodo database that can be accessed through (<https://doi.org/10.5281/zenodo.7378577>) (44).

**ACKNOWLEDGMENTS.** We gratefully acknowledge advice, scientific discussions, and comments on the manuscript from Michael L. Bender. We appreciate Xiangpeng Li, Long Q. Ngo, Li Liu, Junyi Ni, and Tingyuan Liu's assistance during cell culture and harvest, Lili Han for the nutrient measurements, and Sergey Oleynik for maintaining the mass spectrometers at Princeton. This work was funded by the Simons Foundation through award No. 675459 to B.B.W. and was supported by National Natural Science Foundation of China through grants 42125603, 92058204, and 41890802 and by the start-up funding of the University of Oklahoma to W.Q.

Author affiliations: <sup>a</sup>Department of Geosciences, Princeton University, Princeton, NJ 08544; <sup>b</sup>State Key Laboratory of Marine Environmental Science, Xiamen University, Xiamen 361101, China; and <sup>c</sup>Department of Microbiology and Plant Biology, Institute for Environmental Genomics, University of Oklahoma, Norman, OK 73019

- A. E. Santoro, R. A. Richter, C. L. Dupont, Planktonic marine Archaea. *Ann. Rev. Mar. Sci.* **11**, 131-158 (2019).
- W. Martens-Habbena, P. M. Berube, H. Urakawa, J. R. de la Torre, D. A. Stahl, Ammonia oxidation kinetics determine niche separation of nitrifying Archaea and Bacteria. *Nature* **461**, 976-979 (2009).
- E. T. Buitenhuis, P. Suntharalingam, C. Le Quéré, Constraints on global oceanic emissions of  $\text{N}_2\text{O}$  from observations and models. *Biogeosciences* **15**, 2161-2175 (2018).
- A. Freing, D. W. R. Wallace, H. W. Bange, Global oceanic production of nitrous oxide. *Philos. Trans. R. Soc. Lond. B Biol. Sci.* **367**, 1245-1255 (2012).
- Q. Ji, E. Buitenhuis, P. Suntharalingam, J. L. Sarmiento, B. B. Ward, Global nitrous oxide production determined by oxygen sensitivity of nitrification and denitrification. *Global Biogeochem. Cy.* **32**, 1790-1802 (2018).
- C. B. Walker *et al.*, *Nitrosopumilus maritimus* genome reveals unique mechanisms for nitrification and autotrophy in globally distributed marine crenarchaea. *Proc. Natl. Acad. Sci. U.S.A.* **107**, 8818-8823 (2010).
- L. Hink *et al.*, Kinetics of  $\text{NH}_3$ -oxidation, NO-turnover,  $\text{N}_2\text{O}$ -production and electron flow during oxygen depletion in model bacterial and archaeal ammonia oxidisers. *Environ. Microbiol.* **12**, 4882-4896 (2017).
- W. Qin *et al.*, Influence of oxygen availability on the activities of ammonia-oxidizing archaea. *Environ. Microbiol. Rep.* **9**, 250-256 (2017).
- A. E. Santoro, C. Buchwald, M. R. McIlvin, K. L. Casciotti, Isotopic signature of  $\text{N}_2\text{O}$  produced by marine ammonia-oxidizing archaea. *Science* **333**, 1282-1285 (2011).
- J. I. Prosser, L. Hink, C. Gubry-Rangin, G. W. Nicol, Nitrous oxide production by ammonia oxidizers: Physiological diversity, niche differentiation and potential mitigation strategies. *Glob. Chang. Biol.* **26**, 103-118 (2020).
- L. Y. Stein, Insights into the physiology of ammonia-oxidizing microorganisms. *Curr. Opin. Chem. Biol.* **49**, 9-15 (2019).
- L. Y. Stein *et al.*, Comment on "A critical review on nitrous oxide production by ammonia-oxidizing Archaea" by Lan Wu, Xueming Chen, Wei Wei, Yiwen Liu, Dongbo Wang, and Bing-Jie Ni. *Environ. Sci. Technol.* **55**, 797-798 (2021).
- J. A. Kozlowski, M. Stieglmeier, C. Schleper, M. G. Klotz, L. Y. Stein, Pathways and key intermediates required for obligate aerobic ammonia-dependent chemolithotrophy in bacteria and Thaumarchaeota. *ISME J.* **10**, 1836-1845 (2016).
- W. Martens-Habbena *et al.*, The production of nitric oxide by marine ammonia-oxidizing archaea and inhibition of archaeal ammonia oxidation by a nitric oxide scavenger. *Environ. Microbiol.* **17**, 2261-2274 (2015).
- N. Vajrala *et al.*, Hydroxylamine as an intermediate in ammonia oxidation by globally abundant marine archaea. *Proc. Natl. Acad. Sci. U.S.A.* **110**, 1006-1011 (2013).
- M. Y. Jung *et al.*, Indications for enzymatic denitrification to  $\text{N}_2\text{O}$  at low pH in an ammonia-oxidizing archaeon. *ISME J.* **13**, 2633-2638 (2019).
- B. Kraft *et al.*, Oxygen and nitrogen production by an ammonia-oxidizing archaeon. *Science* **375**, 97-100 (2022).
- M. Stieglmeier *et al.*, Aerobic nitrous oxide production through N-nitrosating hybrid formation in ammonia-oxidizing archaea. *ISME J.* **8**, 1135-1146 (2014).
- D. M. Kool, C. Müller, N. Wrage, O. Oenema, J. W. Van Groenigen, Oxygen exchange between nitrogen oxides and  $\text{H}_2\text{O}$  can occur during nitrifier pathways. *Soil Biol. Biochem.* **8**, 1632-1641 (2009).
- N. Wrage, J. W. van Groenigen, O. Oenema, E. M. Baggs, A novel dual-isotope labeling method for distinguishing between soil sources of  $\text{N}_2\text{O}$ . *Rapid Commun. Mass Spectrom.* **19**, 3298-3306 (2005).
- S. Liu *et al.*, Abiotic conversion of extracellular  $\text{NH}_4\text{OH}$  contributes to  $\text{N}_2\text{O}$  emission during ammonia oxidation. *Environ. Sci. Technol.* **51**, 13122-13132 (2017).
- N. Gruber, "The marine nitrogen cycle: Overview and challenges" in *Nitrogen in the Marine Environment*, D. G. Capone, D. A. Bronk, M. R. Mulholland, E. J. Carpenter, Eds. (Elsevier, ed. 2, 2008), pp. 1-50.
- S. Hernández-León, C. Fraga, T. Ikeda, A global estimation of mesozooplankton ammonium excretion in the open ocean. *J. Plankton Res.* **30**, 577-585 (2008).
- F. Breider *et al.*, Response of  $\text{N}_2\text{O}$  production rate to ocean acidification in the western North Pacific. *Nat. Clim. Chang.* **12**, 954-958 (2019).
- J. Charpentier, L. Farias, N. Yoshida, N. Boontanon, P. Raimbault, Nitrous oxide distribution and its origin in the Central and Eastern South Pacific Subtropical Gyre. *Biogeosciences* **4**, 729-741 (2007).
- B. N. Popp *et al.*, Nitrogen and oxygen isotopomer constraints on the origins and sea-to-air flux of  $\text{N}_2\text{O}$  in the plitogrophic Subtropical North Pacific Gyre. *Global Biogeochem. Cy.* **16**, 1064 (2002).
- G. L. Zhang *et al.*, Distribution of concentration and stable isotopic composition of  $\text{N}_2\text{O}$  in the shelf and slope of the Northern South China Sea: Implications for production and emission. *J. Geophys. Res. Oceans* **124**, 6218-6234 (2019).
- C. Frey *et al.*, Regulation of nitrous oxide production in low-oxygen waters off the coast of Peru. *Biogeosciences* **17**, 2263-2287 (2020).
- Q. Ji, B. B. Ward, Nitrous oxide production in surface waters of the mid-latitude North Atlantic Ocean. *J. Geophys. Res. Oceans* **122**, 2612-2621 (2017).
- X. S. Wan *et al.*, Epipelagic nitrous oxide production offsets carbon sequestration by the biological pump. *Nat. Geosci.* **16**, 29-36 (2023).
- C. Frey *et al.*, Kinetics of nitrous oxide production from ammonia oxidation in the Eastern Tropical North Pacific. *Limnol. Oceanogr.* **68**, 424-438 (2022), 10.1002/lno.12283.
- F. Korth, A. Kock, D. L. Arevalo-Martinez, H. W. Bange, Hydroxylamine as a potential indicator of nitrification in the open ocean. *Geophys. Res. Lett.* **46**, 2158-2166 (2019).
- C. Buchwald, K. L. Casciotti, Isotopic ratios of nitrite as tracers of the sources and age of oceanic nitrite. *Nat. Geosci.* **6**, 308-313 (2013).
- K. L. Casciotti, M. McIlvin, C. Buchwald, Oxygen isotopic exchange and fractionation during bacterial ammonia oxidation. *Limnol. Oceanogr.* **55**, 753-762 (2010).
- W. Qin *et al.*, Marine ammonia-oxidizing archaeal isolates display obligate mixotrophy and wide ecotypic variation. *Proc. Natl. Acad. Sci. U.S.A.* **111**, 12504-12509 (2014).
- S. A. Amin *et al.*, Copper requirements of the ammonia-oxidizing archaeon *Nitrosopumilus maritimus* SCM1 and implications for nitrification in the marine environment. *Limnol. Oceanogr.* **58**, 2037-2045 (2013).
- A. Han *et al.*, Nutrient dynamics and biological consumption in a large continental shelf system under the influence of both a river plume and coastal upwelling. *Limnol. Oceanogr.* **57**, 486-502 (2012).

38. M. R. McIlvin, K. L. Casciotti, Fully automated system for stable isotopic analyses of dissolved nitrous oxide at natural abundance levels. *Limnol. Oceanogr.-Meth.* **8**, 54–66 (2010).
39. K. L. Casciotti, D. M. Sigman, M. G. Hastings, J. K. Böhlke, A. Hilkert, Measurement of the oxygen isotopic composition of nitrate in seawater and freshwater using the denitrifier method. *Anal. Chem.* **74**, 4905–4912 (2002).
40. M. A. Weigand, J. Foriel, B. Barnett, S. Oleynik, D. M. Sigman, Updates to instrumentation and protocols for isotopic analysis of nitrate by the denitrifier method. *Rapid Commun. Mass Spectrom.* **30**, 1365–1383 (2016).
41. K. L. Casciotti, J. K. Böhlke, M. R. McIlvin, S. J. Mroczkowski, J. E. Hannon, Oxygen isotopes in nitrite: Analysis, calibration, and equilibration. *Anal. Chem.* **79**, 2427–2436 (2007).
42. M. R. McIlvin, K. L. Casciotti, Method for the Analysis of  $\delta^{18}\text{O}$  in Water. *Anal. Chem.* **78**, 2377–2381 (2006).
43. B. Fry, Steady state models of stable isotopic distributions. *Isotopes. Environ. Health. Stud.* **39**, 219–232 (2003).
44. X. S. Wan *et al.*, Dataset of SCM1 N<sub>2</sub>O production. Zenodo (2022). <https://doi.org/10.5281/zenodo.7378577>. (Deposited 29 November 2022).